Article ID: 1000-324X(2014)10-1110-05 **DOI:** 10.15541/jim20140234

Degradation Effect of Super Acid Modified Fe_2O_3-TiO_2-N on Acrylic Acid under Visible Light

HAN Zhi-Yue, DU Zhi-Ming, ZHANG Ying-Hao, ZHAO Lin-Shuang, CONG Xiao-Min

(State Key Laboratory of Explosion Science and Technology, Beijing Institute of Technology, Beijing 100081, China)

Abstract: Super acid modified Fe_2O_3-TiO_2-N was prepared by hydrolysis precipitation method and sulfuric acid impregnation method. X-ray diffraction (XRD) showed that the catalysts were anatase, Fe_2O_3 were highly decentralized in the catalysts with amorphous form, and modification of SO_4^{2-} inhibited grain growth. Ultraviolet-visible spectra (UV-Vis) showed that Fe and N co-doping made the visible light absorption to the red shift, and sulfuric acid impregnation treatment made the light absorption to the blue shift. Diffuse reflectance Fourier transform infrared (DRIFT-IR) spectra showed that sulfuric acid impregnation can improve the surface acidity of catalysts. X-ray photoelectron spectra (XPS) showed that the valence of S was +6 in the catalysts. Its photocatalytic activity on the degradation of acrylic acid under visible light was studied. The one hour degradation rate of super acid modified Fe_2O_3-TiO_2-N catalyst under visible light was improved 57% than that of the N-doping sample under the same condition.

Key words: co-doping; degradation; visible light; photocatalytic

Nano-TiO_2 is a kind of semiconductor material that is used for many purposes. Its non-toxic, stability, and low price, attract much attention in the study field[1-2]. However, the forbidden band width of TiO_2 is 3.2 eV, so it can only absorb UV light under 387 nm, leading to a low utilization of solar energy. In addition, the combination of electron and hole inspired by light is so easy that the productivity of the carrier is very low. According to the two defects, TiO_2 has been modified by researchers through a variety of methods in order to obtain a better photocatalytic activity. These methods mainly include semiconductor composite, metal doping, nonmetal doping, noble metal deposition and surface superacid treatment, *etc*.

N doped TiO_2 was obtained though calcining TiO_2 in N_2 atmosphere by Asahi[3], and its photocatalytic activity has been proved by experiment. It is considered that hybridization of energy level resulted in that the forbidden band of catalyst became narrow, which enabled the absorption of visible light to the red shift through the calculations of the density function theory. Since then, the researches of N, S, F and C nonmetal ions doped TiO_2 have become a hotspot in the photo catalysis field[4-6]. There are some reported methods about Fe doped TiO_2[7-8]. However, there is no report about N and Fe co-doped TiO_2.

In this paper, superacid modified Fe_2O_3-TiO_2-N was prepared by hydrolysis precipitation method and sulfuric acid impregnation method. The Fe and N co-doping made the absorption of visible light to the red shift and increased the photocatalytic activity in visible light. *In situ* infrared tests showed that sulfuric acid impregnation can improve the surface acidity of catalysts. Its photocatalytic activity on the degradation of acrylic acid under visible light was studied. An hour degradation rate of superacid modified Fe_2O_3-TiO_2-N catalyst in the visible light was 57% more than that of the N-doping sample under the same condition.

1 Experiment

1.1 Preparation of catalysts

1.1.1 Preparation of TiO_2-N

The surfactant lauryl polyoxyethylene ether AEO-3 (0.3vol%) was added to $TiCl_4$ (0.3 mol/L) and stirred vigorously at ambient temperature. The pH of the solution was adjusted to 8–9 with aqueous ammonia. After aging for 16 h, the solution was filtered and washed until all chloride ions were removed. The water in the solution was replaced with absolute ethanol. The resulting alcogel was transferred into a crucible and dried at 50℃. After calcination at 500℃ for 1 h, the TiO_2-N powders were finally obtained.

1.1.2 Preparation of Fe_2O_3-TiO_2-N

The surfactant lauryl polyoxyethylene ether AEO-3 (0.3vol%) was added to $TiCl_4$ (0.3 mol/L) and $Fe(NO_3)_3{\cdot}9H_2O$

Received date: 2014-05-05; **Modified date:** 2014-06-17; **Published online:** 2014-07-20
Biography: HAN Zhi-Yue(1984–), PhD, lecturer. E-mail: hanzhiyue@bit.edu.cn

(0.1 mol/L) with certain proportion, and stirred vigorously at ambient temperature. The pH of the solution was adjusted to 8–9 with aqueous ammonia. After aging for 16 h, the solution was filtered and washed until all chloride ions and nitrate ions were removed. The water in the solution was replaced with absolute ethanol. The resulting alcogel was transferred into a crucible and dried at 50℃. After calcination at 500℃ for 1 h, the powders of Fe_2O_3-TiO_2-N were finally obtained. Calculated with mass concentration, Fe doping amounts were 0.005at%, 0.01at%, 0.05at%, 0.2at% and 0.01at%. The sample with 0.01at% Fe doped was signed as Fe_2O_3-TiO_2-N.

1.1.3 Preparation of Fe_2O_3-TiO_2-N-SO_4^{2-}

The surfactant lauryl polyoxyethylene ether AEO-3 (0.3vol%) was added to $TiCl_4$ (0.3 mol/L) and Fe $(NO_3)_3 \cdot 9H_2O$ (0.1 mol/L) with 0.01at% Fe proportion, and stirred vigorously at ambient temperature. The pH of the solution was adjusted to 8–9 with aqueous ammonia. After aging for 16 h, the solution was filtered and washed until all chloride ions and nitrate ions were removed. The water in the solution was replaced with absolute ethanol. The resulting alcogel was dried at 50℃, and then the solids were impregnated in sulfuric acid with different concentration. After drying at 50℃ and calcination at different temperature for 1 h, the powders were finally obtained. The impregnated concentrations of sulfuric acid were 0.2, 0.5, 0.8 and 1.0 mol/L. The sample with 0.8 mol/L impregnated concentration was signed as Fe_2O_3- TiO_2-N-SO_4^{2-}.

1.2 Measurements

1.2.1 Characterization

X-ray diffraction (XRD) measurements were performed by using a Shimadzu HR6000X (Cu target X tube, voltage 40.0 kV, current 30.0 mA). Diffuse reflectance fourier transform infrared (DRIFT-IR) spectra were recorded by a Prestige-21IR spectrophotometer with KBr pellet. X-ray photoelectron spectroscopy (XPS) analyses were conducted by an ESCALAB 250, which tested the electronic binding energy of the samples. UV-visible spectra were measured by using a Hitachi U-3010 spectrophotometer.

1.2.2 Evaluation of photo catalytic activity

The photo catalytic activities of the synthesized catalysts were examined using a self-designed photo catalytic reaction apparatus (Fig. 1), which consists of a double-layered cylindrical quartz flask with a visible lamp (18 W, wavelengths: 420 nm, intensity: 12000 μW/cm^2). Acrylic acid aqueous solution (300 mL, 100 mg/L) is used as degradation solution. The dosage of catalyst was 0.5 g. The air was introduced from the bottom of the reaction solution at the rate of 30 mL/min and the temperature was maintained at (25±1)℃. Continuous stirring ensured that catalysts were dispersed evenly in the reaction solution. A certain volume of the reaction solution was analyzed periodically after each visible lamping for 6 h. The absorbance of these solutions after centrifugation was measured at 210 nm by UV-Vis spectrophotometer (752 B). The photocatalytic activities were estimated by the degradation rate of acrylic acid.

2 Results and discussion

2.1 XRD

XRD patterns for the TiO_2-N, Fe_2O_3-TiO_2-N and Fe_2O_3-TiO_2-N-SO_4^{2-} powers are shown in Fig. 2. In XRD patterns of TiO_2 particles, the peaks at 25.32°, 37.84°and 48.2° are assigned to the (101), (004) and (200) lattice planes, which are attributed to the signals of theanatase phase. There is no Fe, N and S diffraction peaks in the XRD patterns of samples, indicating the doping elements are dispersed in TiO_2 with a high degree form. The treatments of Fe doping and sulfuric acid impregnation can significantly inhibit the growth of TiO_2 grain to a certain extent, and XRD diffraction peak intensity of treated samples becomes weak.

The XRD patterns of samples treated by sulfuric acid and calcined at different temperatures are shown in Fig. 3. Calcination temperatures have little effects on the crystal phase of the samples from 400–700 ℃. All the treated samples are anatase. However, crystal diffraction peak intensity increases and the peaks become sharp as the increase of temperature. This indicates that there is no crystal change after calcination, the crystal structure becomes complete, and the grain grows up.

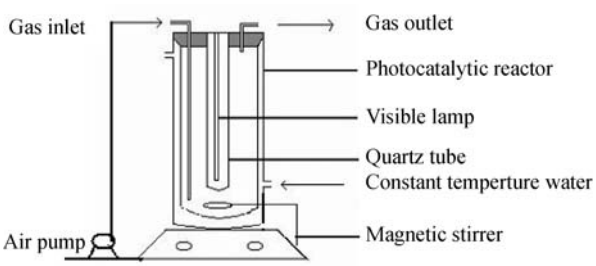

Fig. 1　Catalytic reactor system for degradation of acrylic acid with visible lamp irradiation

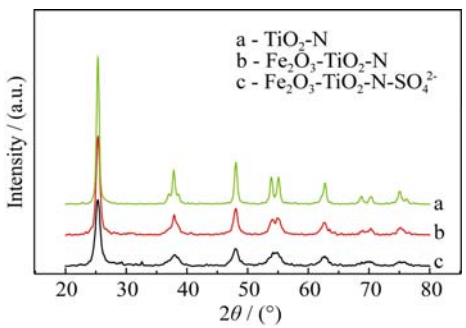

Fig. 2　XRD patterns of the TiO_2-N, Fe_2O_3-TiO_2-N and Fe_2O_3-TiO_2-N-SO_4^{2-} powders

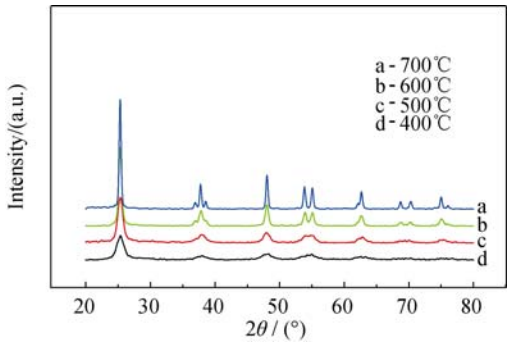

Fig. 3 XRD patterns of samples treated by sulfuric acid and calcined at different temperatures

2.2 DRIFT

DRIFT spectroscopy associated with NH_3 adsorption is a powerful technique for investigating the surface acidity of materials[9]. Fig. 4 presents a comparison of surface acidity of samples treated by sulfuric acid with different concentration. The bands at 1513 cm^{-1} are usually attributed to the L-acid sites, while the one at 1690 cm^{-1} can be assigned to the B-acid sites. It is clearly shown from Fig. 4 that the amount of surface acidity increases with the concentration of sulfuric acid increases. When the concentration of sulfuric acid is 1 mol/L, the amount of surface acidity is the strongest.

2.3 XPS

Figures 5, 6 and 7 are the high-resolution XPS spectra of Fe_2O_3-TiO_2-N-SO_4^{2-}. Figure 5 shows the narrow scans for the S2p peaks locate at 168.55 eV, which is attributed to auger electron peak of S^{6+}[10]. This indicates that SO_4^{2-} combined on the surface of TiO_2 with the form of chelate double coordination, which results in that the amount of surface acidity increases and the photo catalytic activity is improved. There is no peak locates at 162 eV, which is attributed to auger electron peak of S^{2-}[10]. This indicates that S does not dope into the TiO_2 lattice to replace O.

Figure 6 shows the narrow scans for the N peaks. There are two nitrogen peaks at 399.7 and 402 eV. The former is attributed to N–Ti–O. The latter is attributed to N in the

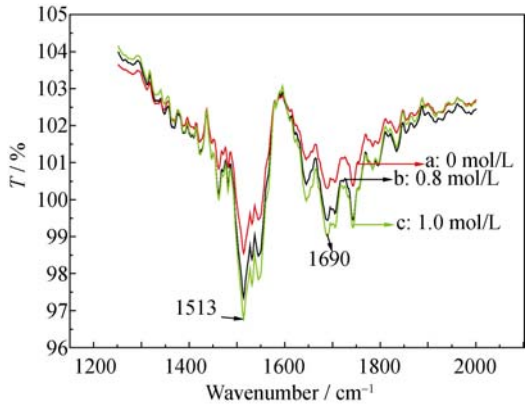

Fig. 4 DRIFT spectroscopy associated with NH_3 adsorption on catalysis with different concentrations of H_2SO_4

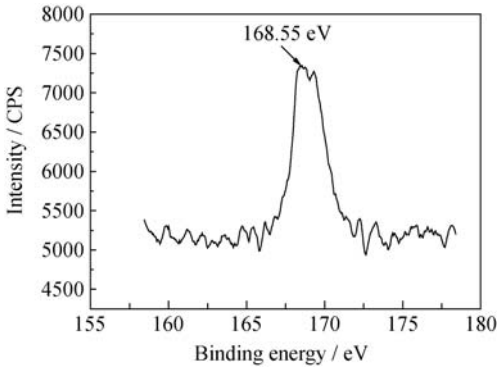

Fig. 5 S XPS patterns of Fe_2O_3-TiO_2-N-SO_4^{2-}

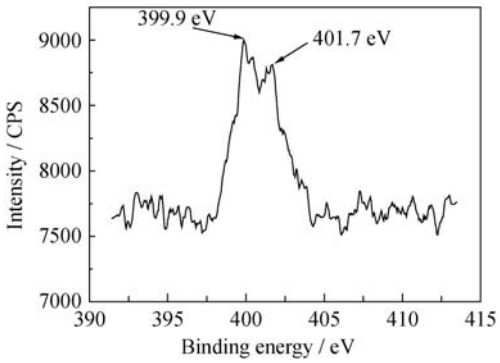

Fig. 6 N XPS patterns of Fe_2O_3-TiO_2-N-SO_4^{2-}

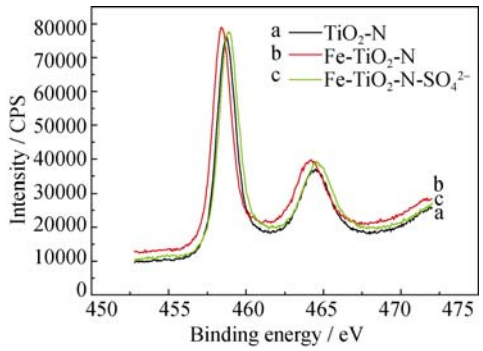

Fig. 7 Ti XPS patterns of Fe_2O_3-TiO_2-N-SO_4^{2-}

chemical adsorption state. N doping decreases the forbidden band width of TiO_2, and expands the spectral response of the catalyst to visible light, so it improves the photo catalytic activity of the catalyst. In addition, N doping makes oxygen defect appears on the TiO_2 surface[11], which is beneficial to the activity in visible light. Fe concentration is too low, so there is no Fe peak shown on the XPS. All in all, synergies of N, S doping improve the catalyst activity of Fe_2O_3-TiO_2-N-SO_4^{2-}.

Figure 7 shows the narrow scans for the Ti2p peaks. The binding energy of Ti2p becomes lower after Fe doping, but the binding energy of Ti2p becomes higher after sulfuric acid impregnation. The increase of Ti2p binding energy indicates that the electropositivity of titanium ions on the catalyst surface increases. The changes of the chemical state on the surface improve the oxygen adsorption capacity of catalyst surface, and reduce the combination rate of e^--h^+.

Adsorption ability of catalyst greatly increases, leading to the photo catalytic activity of catalyst being improved.

2.4 UV-Vis

The UV-Vis spectra of samples are shown in Fig. 8. Compared with pure TiO_2, there are certain red shifts of catalysts in different degree. The order of redshift degree is: Fe_2O_3-TiO_2-N>TiO_2-N> Fe_2O_3-TiO_2-N-SO_4^{2-}. The N doping formed O–Ti–N, which formed the doping energy level. Therefore, a redshift to the visible region occurs in the UV-visible spectrum of TiO_2-N sample. Fe_2O_3 is a narrow band gap semiconductor. Its forbidden band width is 2.2 eV. A small amount of Fe_2O_3 doping enables the electron transition path changes, so a redshift to the visible region occurs after Fe doping.

2.5 Determination of photocatalytic activity

2.5.1 The photocatalytic activity of samples

The degradation rates of target in 1 h of samples are shown in Fig. 9. According to the degradation rate of target in 1 h, the order of photo catalytic activity is: sample c> sample b> sample a>P25. The degradation rate of Fe_2O_3-TiO_2-N-SO_4^{2-} (c) is 46.98%. The degradation rate of P25 is 29.05%, which is the lowest.

Visible light response of prepared samples is better than that of P25, so the photocatalytic activity of Samples a, b and c are higher than that of p25. The sulfuric acid impregnation improves the surface acidity and reduces the size of catalysts, so the photocatalytic activity of sample c is the highest.

2.5.2 The influence of the sulfuric acid concentration on photocatalytic activity

The degradation rates with samples treated by different sulfuric acid concentration are shown in Fig. 10. The degradation rate increases with the increase of sulfuric acid concentration within the concentration range in 0–0.8 mol/L. When the sulfuric acid concentration is 0.8 mol/L, the degradation rate is 46.98%, and the photocatalytic activity is the highest. This is because when the impregnation concentration is too low, the content of sulfur and acidity is too low in the catalyst, which results in the low photocatalytic activity. If the sulfuric acid concentration contin ues to increase, the degradation rate declines. This is because when the im pregnation concentration is too high, sulfate can form on the surface easily, which can cover the activities, so it can affect the activity of catalysts and the degradation rate of acrylic acid.

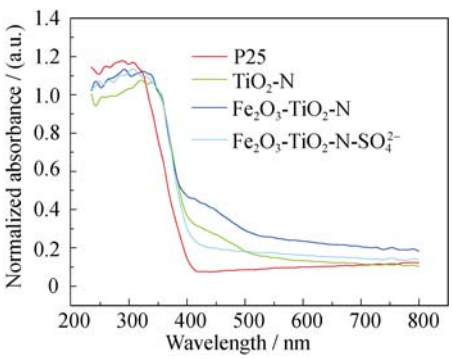

Fig. 8　UV-Vis absorption of different samples

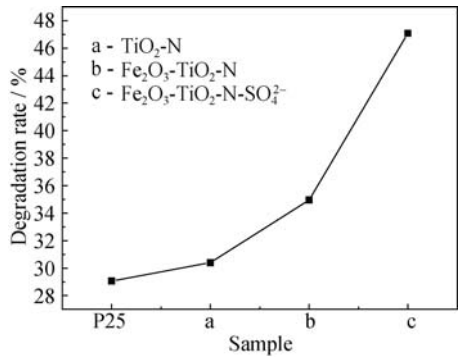

Fig. 9　Degradation rate of acrylic acid with different catalysts

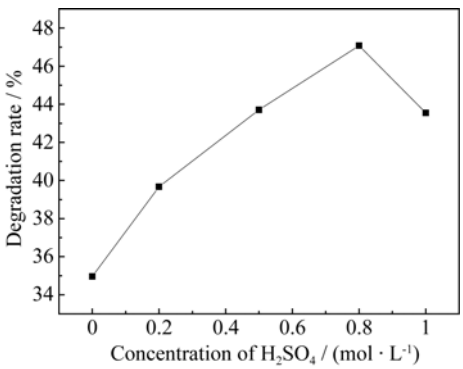

Fig. 10　Degradation rate of acrylic acid with different concentrations of sulfuric acid

2.5.3 The influence of calcination temperature on photocatalytic activity

The degradation rates of samples treated by different calcination temperature are shown in Fig. 11. The degradation rate increases with the increase of calcination temperature. When the calcination temperature is 500 ℃, thedegradation rate is 46.98%, and the photocatalytic activity is the highest. If the calcination temperature further increases, the degradation rate declines. When the calcination temperature is lower than 500℃, some organic matters (such as alcohols, surfactants) are coated on the surface of catalysts, so the catalytic active centers are covered. As the increase of calcination temperature, impurities on the surface of catalysts are broken down or desorption, so the active centers on the catalyst surface increase, and then the activity of catalysts increases. However, the particle sizes of catalysts become large as the temperature increases, so the catalytic activity of catalysts declines when the temperature is higher than 500℃.

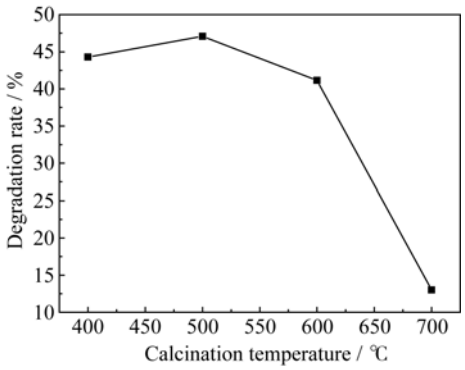

Fig. 11 Degradation rate of acrylic acid with different calcination temperatures

3 Conclusions

Super acid modified Fe_2O_3-TiO_2-N was prepared by hydrolysis precipitation method and sulfuric acid impregnation method firstly. The Fe and N co-doping enables the visible light absorption to the red shift and increases the photo catalytic activity. Sulfuric acid impregnation inhibits grain growth and improves the surface acidity of catalysts. When the Fe doping amount is 0.01at% and the impregnation concentration of sulfuric acid is 0.8 mol/L, the degradation rate is 46.98%, and the photocatalytic activity is the highest.

References:

[1] FUJISHIMA A, HONDA K. Electrochemical photolysis of water at a semiconductor electrode. *Nature*, 1972, **238(5358):** 37–38.

[2] FUJISHIMA A, RAO T, TRYK D. Titanium dioxide photocatalysis. *Journal of Photochemistry and Photobiology C: Photochemistry Reviews*, 2000, **1(1):** 1–21.

[3] ASAHI R, MORIKAWA T, OHWAKI T, *et al*. Visible-light photocatalysis in nitrogen-doped titanium oxides. *Science*, 2001, **293 (5528):** 269–271.

[4] UMEBAYASHI T, YAMAKI T, ITOH H, *et al*. Band gap narrowing of titanium dioxide by sulfur doping. *Applied Physics Letters*, 2002, **81(3):** 454–456.

[5] YU J C, YU J G, HO W K, *et al*. Effects of F^- doping on the photocatalytic activity and microstructures of nanocrystalline TiO_2 powders. *Chemistry of Materials*, 2002, **14:** 3808–3816.

[6] SAKTHIVEL S, KISCH H. Daylight photocatalysis by carbon modified titanium dioxide. *Angew. Chem. Int. Ed.*, 2003, **42(40):** 4908–4911.

[7] Mwangi I W, Ngila J C, Ndungu P, *et al*. Immobilized Fe (III)-doped titanium dioxide for photodegradation of dissolved organic compounds in water. *Environmental Science and Pollution Research*, 2013, **20(9):** 6028–6038.

[8] YALCIN Y, KILIC M, CINAR Z. Fe^{+3}-doped TiO_2: A combined experimental and computational approach to the evaluation of visible light activity. *Applied Catalysis B: Environmental*, 2010, **99(3/4):** 469–477.

[9] LEE SEUNG JOON, HAN SANG WOO, YOON MINJOONG, *et al*. Adsorption characteristics of 4-dimethylaminobenzoic acid on silver and titania: diffuse reflectance infrared Fourier transform spectroscopy study. *Vibrational Spectroscopy*, 2000, **24(2):** 265–275.

[10] GOLE J L, STOUT J D, BURDA C, *et al*. Highly efficient formation of visible light tunable $TiO_{2-x}N_x$ photocatalysts and their transformation at the nanoscale. *The Journal of Physical Chemistry B*, 2004, **108(4):** 1230–1240.

[11] IHARA T, MIYOSHI M, IRIYAMA Y, *et al*. Visible-light-active titanium oxide photocatalyst realized by an oxygen-deficient structure and by nitrogen doping. *Applied Catalysis B: Environmental*, 2003, **42:** 403–409.

超强酸化 Fe_2O_3-TiO_2-N 在可见光下降解丙烯酸的研究

韩志跃，杜志明，张英豪，赵林双，丛晓民

(北京理工大学 爆炸科学与技术国家重点实验室，北京 100081)

摘 要: 通过水解沉淀法和 H_2SO_4 浸渍干凝胶的方法，制备了具有可见光活性的超强酸化的 Fe_2O_3-TiO_2-N 光催化剂。XRD 测试结果表明，所制得的催化剂为锐钛矿型，且 H_2SO_4 处理显著抑制了晶粒的长大。UV-Vis 分析表明，N、Fe 掺杂样品相比纯 TiO_2 有一定的红移，而浸渍硫酸的处理使样品的光吸收蓝移。原位红外的测试表明，H_2SO_4 浸渍提高了催化剂的表面酸性，XPS 测试说明了 S 以+6 价存在于催化剂中。对丙烯酸的光降解试验表明，相比单独 N 掺杂的 TiO_2，所得的超强酸化的 Fe、N 共掺杂光催化剂活性提高了 57%。

关 键 词: 共掺杂；降解；可见光；光催化

中图分类号: TQ174 **文献标识码:** A